



HAL
open science

Left Hand dispersion of a stack of sub-wavelength hole metal arrays at terahertz frequencies

Charles Croënne, F. Garet, Eric Lheurette, J.-L. Coutaz, D. Lippens

► **To cite this version:**

Charles Croënne, F. Garet, Eric Lheurette, J.-L. Coutaz, D. Lippens. Left Hand dispersion of a stack of sub-wavelength hole metal arrays at terahertz frequencies. *Applied Physics Letters*, 2009, 94, pp.133112. hal-00597580

HAL Id: hal-00597580

<https://hal.science/hal-00597580>

Submitted on 7 Sep 2021

HAL is a multi-disciplinary open access archive for the deposit and dissemination of scientific research documents, whether they are published or not. The documents may come from teaching and research institutions in France or abroad, or from public or private research centers.

L'archive ouverte pluridisciplinaire **HAL**, est destinée au dépôt et à la diffusion de documents scientifiques de niveau recherche, publiés ou non, émanant des établissements d'enseignement et de recherche français ou étrangers, des laboratoires publics ou privés.

Left handed dispersion of a stack of subwavelength hole metal arrays at terahertz frequencies

Charles Croënne,¹ Frédéric Garet,² Éric Lheurette,¹ Jean-Louis Coutaz,² and Didier Lippens^{1,a)}

¹*Institut d'Électronique, de Microélectronique et Nanotechnologies, Université des Sciences et Technologies de Lille, Avenue Poincaré BP 60069, 59652 Villeneuve d'Ascq Cedex, France*

²*Laboratoire IMEP-LAHC, UMR 5130 du CNRS, Université de Savoie, 73376 Le Bourget du Lac Cedex, France*

(Received 6 February 2009; accepted 13 March 2009; published online 3 April 2009)

We report on the electromagnetic response of a stack of subwavelength hole metal arrays. The samples were designed for exhibiting left handed dispersion branches under normal incidence, and their transmissivities were optimized via the fabrication of elliptical-shaped holes. They are constituted of benzocyclobutene layers with tens of micron thicknesses and submicron-thick gold films patterned by photolithography. Experimental evidence, achieved by time-domain terahertz spectroscopy and supported by full wave simulations, of a ground left handed dispersion branch is found around 0.45 THz. The insertion losses are -3 dB for a five-layer structure, this good level being explained by the matching of the impedance. © 2009 American Institute of Physics.

[DOI: [10.1063/1.3114411](https://doi.org/10.1063/1.3114411)]

After the story of edge-illuminated left handed three dimensional metamaterials fabricated from split ring resonator and wire arrays,¹ operating satisfactorily at least up to 100 GHz,² most of the current research effort is now oriented toward the fabrication of metamaterials that can operate in the infrared spectral region under normal incidence. Ideas to reach this goal are numerous, starting from the pioneering work of Podolskiy³ who proposed to stack two nanoresonators coupled in the direction of wave propagation. Within this scheme, the proper condition of the magnetic field polarization, i.e., perpendicular to the planar resonators, can be fulfilled. The so-called fishnet structure⁴⁻⁶ is derived from the same idea. On the other hand, subwavelength hole metal arrays have also shown the possibility to observe enhanced transmission.⁷⁻⁹ *A priori*, their operating principle is based on the effect of extraordinary transmission through a subwavelength hole single grid comparable to a frequency selective surface. In the infrared, the operation of such a grid is based on surface plasmon (SP) physics, and no evidence of negative index was demonstrated for a single array. Recently, the demonstration of the operation of such a grid at millimeter wave shows that the SP propagation condition was not necessary to explain the electromagnetic properties due to the fact that the hole structuring permits to mimic surface wave.¹⁰ More importantly, it was shown by the Navarre University group¹¹ that a left handed dispersion can also be observed when two grids at least are stacked, which is also the requirement for a fishnet approach. Obviously there are close similarities between the coupled metal rod arrays and the metal structure obtained by taking the complementary arrangement of the staked hole arrays according to the Babinet principle.

In the present paper, we go further with the possibility to induce a negative effective refractive index by means of a stack of hole arrays under normal incidence. This work

shows two key originalities with respect to the state of the art in this field. The first original point concerns the frequency of operation, in the terahertz (THz) frequency range and thus one order of magnitude higher than the operating frequency reported in Ref. 11 around 55 GHz. This increase in the operating frequency will not modify the main conclusion drawn at lower frequency, namely, the fact that SPs do not explain the singular electromagnetic properties of these structures, notably a negative value of refractive index. However the aspect ratio between the dielectric layers and the metallic films, which form the stack of subwavelength hole arrays, is strongly modified with values as close to 100. As a consequence, there is a strong unbalance between surface modes in the dielectric layer and guided modes in the holes. The other challenges are (i) in the fabrication of the samples, which requires using microelectronics technologies, and (ii) in the characterization by means of coherent terahertz time domain spectroscopy (THz-TDS) in order to describe the effects of phase advance. The second original issue is the achievement of moderate insertion losses despite the fact that intrinsic losses of both dielectric and metal materials increase at higher operation frequencies. We show that such a result is not connected to the fact that the operation behavior can be compared to a transmission line approach as proposed in the literature.¹²

In our case, it is believed that a matching of the impedance close to the pass band edge is responsible for such a high transmission level at the detriment however of the band width. To achieve such a high transmissivity, an optimization of the hole shape with an elliptical configuration was performed in a manner similar to the width optimization of the strips of fishnet structures.

Figures 1(a) and 1(b) show a large scale photograph and an optical microscope view of the top metal layer. The shape of the hole is elliptical with a ratio of 1.7:1 between the large and small axes. The patterning of holes in the metal film, deposited by evaporation with a Plassys MEB 550S equipment on a GaAs semi-insulating substrate, was achieved by

^{a)}Author to whom correspondence should be addressed: Electronic mail: didier.lippens@iemn.univ-lille1.fr

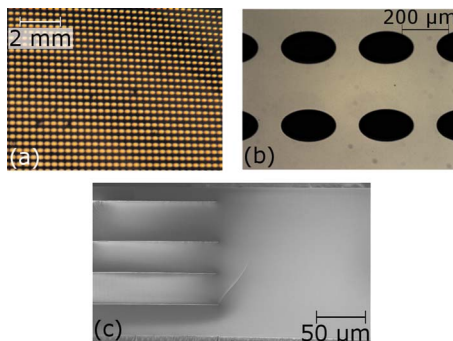


FIG. 1. (Color online) (a) View of one part of the array. (b) Optical microscope view and (c) SEM view of the cross section of the stack of metallic arrays. The homogeneous region on the right corresponds to the cross section of the elliptical holes.

lift-off photolithography using a Clariant AZnLOF 2070 negative resist.

The dielectric spacers are benzocyclobutene (BCB) resist layers. BCB, supplied by the Dow Chemical Co., was chosen for its moderate loss in the terahertz frequency range. Its permittivity constant given by the supplier is 2.6 with a loss tangent ranging from 0.005 to 0.01 at 1 THz. A parametric numerical study of the influence of the BCB thickness on the electromagnetic properties of the device has orientated our choice toward a few tens of micron BCB thickness, hence much thicker than the metal films contrary to the devices fabricated for microwaves applications.¹¹ The BCB layers were deposited by spin coating and subsequently annealed under nitrogen controlled atmosphere at a temperature of around 300 °C. In practice, we faced two difficulties: (i) the high strain of the BCB layer so that only a limited number of layers (here $n \leq 5$) were deposited with a reasonable bowing of the substrate and (ii) a relatively large dispersion in the BCB thickness measured from the cross section of a peeled sample piece. A scanning electron microscope (SEM) picture of this cross section is shown in Fig. 1(c); the thicknesses range from 30.9 to 44.1 μm . Finally to suppress the substrate effects that introduce an asymmetry in the sample boundaries (interfaced with air on the one side and with a semiconductor on the other side), a membranelike structure was fabricated. This was realized by means of a deep backside wet chemical etching ($\text{H}_2\text{SO}_4:\text{H}_2\text{O}_2:\text{H}_2\text{O}$), the multilayer playing the role of an etch stop layer.

The transmission measurements were performed with a classical THz-TDS setup using low temperature grown-GaAs photoswitches as antennas, which was already described elsewhere.¹³ The frequency spectrum of the signals delivered by this setup, as obtained by a Fourier-transform of the temporal waveforms, ranges from 0.1 to 5 THz. At the top of the spectrum amplitude, i.e., in between 0.5 and 1 THz, the measured dynamics is 60 dB. At the sample location, the THz beam is made almost parallel (3 cm waist at 1 THz) by means of parabolic mirrors. To avoid spurious effect due to diffraction at the sample edges, a 2 cm diameter diaphragm was located in front of the sample, leading to the illumination of about 2700 cells. Despite the fact that the terahertz beam delivered by the photoswitch is almost polarized,¹⁴ a fine control of the polarization state (the E -polarization state corresponds to the E -field directed along the small axis of the elliptical holes) was realized with grid polarizers. The experimental frequency resolution is 3.75 GHz since the maxi-

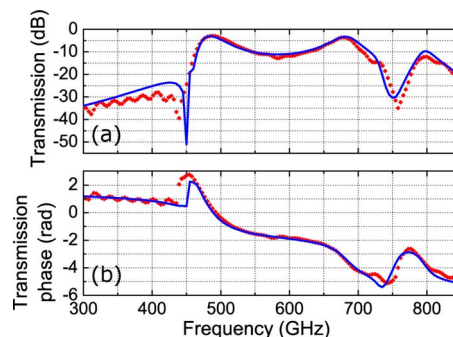


FIG. 2. (Color online) Simulated (solid blue/black lines) and measured (red/gray diamonds) transmission spectra in magnitude (a) and phase (b) for the sample in Fig. 1.

mum delay of the delay line is 266 ps. The terahertz response presented below is obtained by differential measurement with and without the sample in the terahertz beam path.

Figure 2 shows the frequency dependences of the magnitude and of the phase of the transmission coefficient (T). The key feature in the magnitude of T is the presence of a pass band above 0.45 THz, this frequency corresponding to an antiresonance state (zero of transmission). Below this characteristic frequency, the transmissivity of the sample is extremely weak (of the order of -30 dB) as the hole array is operating below the hole cutoff. From the hole dimensions and taking into account its elliptical shape, as well as the BCB index, one can estimate this cutoff frequency to approximately 483 GHz. This means that the sample exhibits an extraordinary transmission in the sense that a pass band is experimentally evidenced in a frequency band below the conventional Bethe limitation¹⁵ as discussed above. By considering now the unwrapped phase, it can be noticed that the phase offset measured with and without the sample is positive in the first pass band, which indicates that the refractive index is negative.

We also plotted in Fig. 2 the calculated frequency dependence of the transmission in modulus and phase, which can be obtained by a full wave analysis. The calculation was performed by means of the Maxwell equation solver HIGH FREQUENCY STRUCTURE SIMULATOR by Ansoft. In these calculations, the metal losses were taken into account with a conductivity of the gold films of 4.1×10^7 S/m. Losses of the BCB layers, with values of loss tangents ranging from 0.01 to 0.03 at 800 GHz, were also included in the simulation. At last, the dispersion in the BCB layer thickness, evidenced in the cross section displayed in Fig. 1(c), was also taken into account. Under these conditions, it can be noted that there is an excellent fit between the measured and the experimental data. Some discrepancies exist in the upper part above 850 GHz (not shown here) where pronounced dips can be evidenced in the plot of the numerical results but are not reproduced in the experimental trace. They are attributed to Wood anomalies whose analysis is beyond the scope of the present work.

This excellent fit below 850 GHz permitted us to get a deeper insight into the electromagnetism of the structure by the retrieval of the dispersion characteristic and of the frequency dependence of the impedance. The results are reported in Fig. 3. They were obtained by a Fresnel inversion technique, which was applied in our group for describing metamaterials as well as photonic crystals.¹⁶ For the stop

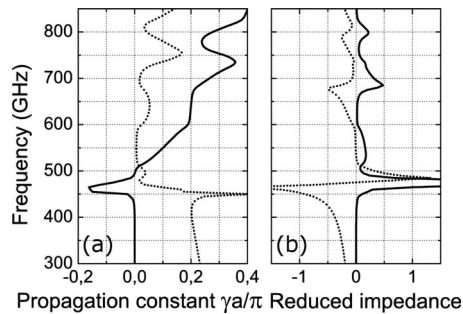


FIG. 3. Dispersion diagram with the real (dotted line) and imaginary (solid line) parts of the propagation constant. (b) Frequency dispersion of the real (solid line) and imaginary (dotted line) parts of the reduced impedance.

band, notably the forbidden band below 450 GHz, the figure of interest is the attenuation constant corresponding to the imaginary part of the wavevector amplitude k . For the left handed branch between 450 and 480 GHz, the dispersion was plotted for the negative value of the real part of k . It can be verified that in this band, the group velocity that corresponds to the slope of the $\omega(k)$ function is positive, while the phase velocity $v_p = \omega/k$ is negative. Above 480 GHz, a narrow gap can be seen before the conventional right handed branch, which starts around 510 GHz. It is believed that a pure balanced composite metamaterial that exhibits negative zero positive index¹⁷ could be achieved by a proper design. With respect to the normalized impedance it can be seen that the matching of the real impedance ($z=1$) was achieved close to the narrow stop band edge, explaining the high transmissivity peak at a frequency of about 470 GHz.

In conclusion, an experimental evidence of a ground left handed transmission branch, which thus corresponds to a negative refractive index, was demonstrated by a THz-TDS analysis of a stack of subwavelength hole arrays. Despite the

fact that the intrinsic dielectric and metal losses lower the maximum of transmission, it appears that the key feature for achieving a high transmission level stems from the characteristic impedance matching, which was obtained here close to the stop band edge.

This work was carried out in the framework of a Délégation Générale pour l'Armement contract.

- ¹R. A. Shelby, D. R. Smith, and S. Schultz, *Science* **292**, 77 (2001).
- ²F. Zhang, D. P. Gaillot, C. Croënne, E. Lheurette, X. Mélique, and D. Lippens, *Appl. Phys. Lett.* **93**, 083104 (2008).
- ³V. A. Podolskiy, A. K. Sarychev, and V. M. Shalaev, *J. Nonlinear Opt. Phys. Mater.* **11**, 65 (2002).
- ⁴S. Zhang, W. Fan, K. J. Malloy, S. R. J. Brueck, N. C. Panoiu, and R. M. Osgood, *Opt. Express* **13**, 4922 (2005).
- ⁵S. Zhang, W. Fan, N. C. Panoiu, K. J. Malloy, R. M. Osgood, and S. R. J. Brueck, *Phys. Rev. Lett.* **95**, 137404 (2005).
- ⁶G. Dolling, C. Enkrich, M. Wegener, C. M. Soukoulis, and S. Linden, *Science* **312**, 892 (2006).
- ⁷J. Rivas, C. Schotsch, P. H. Bolivar, and H. Kurz, *Phys. Rev. B* **68**, 201306 (2003).
- ⁸M. Beruete, M. Sorolla, I. Campillo, J. S. Dolado, L. Martin Moreno, J. Bravo-Abad, and F. J. Garcia-Vidal, *Opt. Lett.* **29**, 2500 (2004).
- ⁹A. G. Schuchinsky, D. E. Zelenchuk, and A. M. Lerer, *J. Opt. A, Pure Appl. Opt.* **7**, S102 (2005).
- ¹⁰A. Mary, S. G. Rodrigo, F. J. Garcia-Vidal, and L. Martin-Moreno, *Phys. Rev. Lett.* **101**, 103902 (2008).
- ¹¹M. Beruete, M. Sorolla, and I. Campillo, *Opt. Express* **14**, 5445 (2006).
- ¹²F. Medina, F. Mesa, and R. Marqués, *IEEE MTT-S Int. Microwave Symp. Dig.* **2008**, 213.
- ¹³F. Aquistapace, L. Duvillaret, F. Garet, J.-F. Roux, and J.-L. Coutaz, *J. Appl. Phys.* **94**, 7888 (2003).
- ¹⁴F. Garet, L. Duvillaret, and J.-L. Coutaz, *Proc. SPIE* **3617**, 30 (1999).
- ¹⁵H. A. Bethe, *Phys. Rev.* **66**, 163 (1944).
- ¹⁶C. Croënne, N. Fabre, D. P. Gaillot, O. Vanbésien, and D. Lippens, *Phys. Rev. B* **77**, 125333 (2008).
- ¹⁷F. Zhang, G. Houzet, E. Lheurette, D. Lippens, M. Chaubet, and X. Zhao, *J. Appl. Phys.* **103**, 084312 (2008).